High-Performance Solid Acid Fuel Cells Through Humidity Stabilization

Dane A. Boysen, Tetsuya Uda, Calum R. I. Chisholm, Sossina M. Haile*

Although they hold the promise of clean energy, state-of-the-art fuel cells based on polymer electrolyte membrane fuel cells are inoperable above 100°C, require cumbersome humidification systems, and suffer from fuel permeation. These difficulties all arise from the hydrated nature of the electrolyte. In contrast, "solid acids" exhibit anhydrous proton transport and high-temperature stability. We demonstrate continuous, stable power generation for both H_2/O_2 and direct methanol fuel cells operated at ~250°C using a humidity-stabilized solid acid CsH_2PO_4 electrolyte.

Solid acid compounds comprise hydrogen-bonded oxyanions, often tetrahedral (such as SO_4, SeO_4, PO_4, and AsO_4), and metal cations, which provide overall charge balance to the hydrogen bond network. Several solid acids exhibit an ordered arrangement of hydrogen bonds at room temperature and, upon slight heating, become structurally disordered. A typical example is $CsHSO_4$, which transforms from a monoclinic to a tetragonal structure at 141°C (*1*). Accompanying this transformation is an increase in proton conductivity of two to three orders of magnitude, reaching values as high as 10^{-2} ohm^{-1} cm^{-1}. Both the transition and the ion transport are commonly referred to as "superprotonic." Fuel cell operation at the slightly elevated temperatures enabled by superprotonic solid acids relaxes the purity requirements on the hydrogen fuel in a hydrogen/air fuel cell, increases the activity of the catalysts, provides useful waste heat for cogeneration configurations, and, particularly important for automotive applications, reduces the size of the radiator. Moreover, unlike polymers, solid acids exhibit anhydrous proton transport, and thus, careful water management to remove water from the cathode and replenish it at the anode is not necessary. For direct methanol fuel cell (DMFC) applications, the solid, water-free nature of the electrolyte raises the possibility of fuel-impermeable membranes.

The implementation of known superprotonic solid acids in fuel cells has been hindered by their water solubility and poor mechanical behavior. Despite these properties, successful operation of $CsHSO_4$-based fuel cells has been demonstrated (*2*). The key to this success was operating the fuel cells above 100°C; at these temperatures, H_2O is present in the form of steam and is thus harmless to the otherwise water-soluble electrolyte. A greater obstacle, recently recognized, arises from the catalyzed reduction of sulfate and selenate solid acids under hydrogen atmospheres (*3*). Accordingly, in this work, we investigated the viability of CsH_2PO_4 as an electrolyte in solid acid fuel cells. A phosphate-based compound is not expected to suffer a reduction reaction to form solid phosphorus or gaseous H_xP species. Thermal analysis of CsH_2PO_4 (Fig. 1) confirms this expectation (*4*). Thermal decomposition of CsH_2PO_4, even when mixed with a Pt catalyst, is independent of whether the atmosphere is reducing (Fig. 1A) or oxidizing (Fig. 1B). In both cases, weight loss begins at 223°C, and is due entirely to dehydration, as evident from analysis of the evolved gas (that is, no phosphate fragments were detected). It has been proposed that the dehydration reaction proceeds by means of the formation of amorphous hydrogen pyrophosphate and polyphosphate intermediates until complete decomposition to $CsPO_3$ occurs (*5*), as shown by reaction 1.

$$CsH_2PO_4(s) \rightarrow CsH_{2-2x}PO_{4-x}(s) + xH_2O(g),\ (0 < x \leq 1) \quad (1)$$

Controversy over the superprotonic phase transition behavior in CsH_2PO_4 has recently been resolved (*6*). At atmospheric pressures and very slow heating rates, dehydration precedes and often masks a superprotonic transition, and has been the source of reported discrepancies. The data collected here reveal a structural transition at 238°C, superposi-

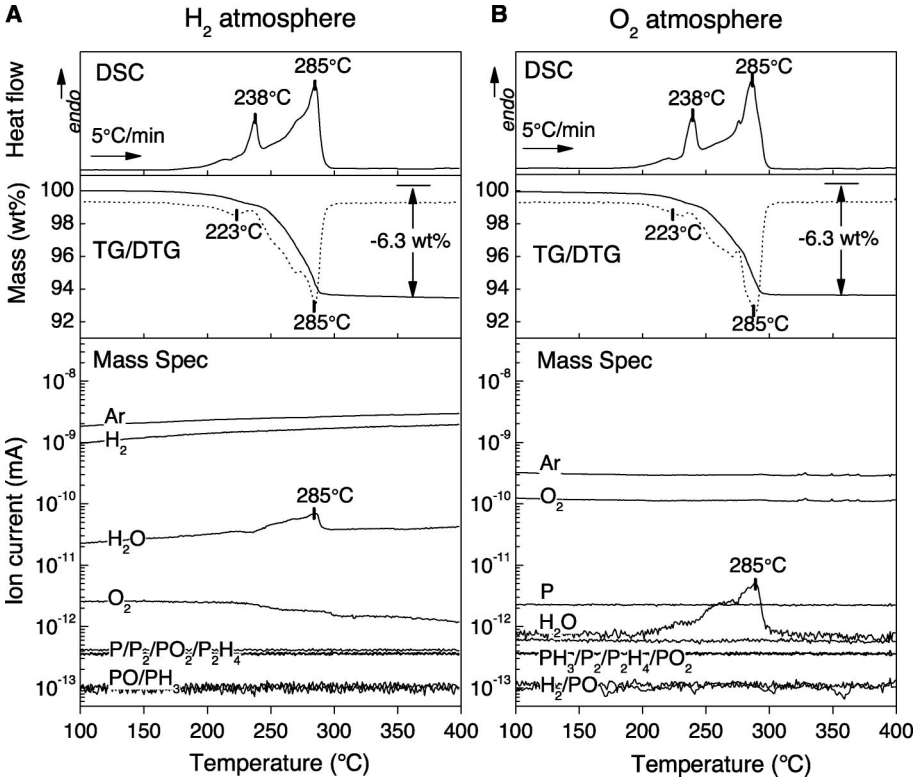

Fig. 1. Thermal analysis of CsH_2PO_4 under (**A**) H_2 and (**B**) O_2 atmospheres. Thermal characterization of CsH_2PO_4 powder mixed with Pt-black (4:1 weight ratio) upon heating to 400°C at 5°C min^{-1} by simultaneous differential scanning calorimetry (DSC) (top) and by thermalgravimetry and differential thermalgravimetry (TG/DTG) (middle), with off-gases analyzed by mass spectrometry (Mass Spec) (bottom) under (A) 96 volume % Ar and 4 volume % H_2 flowing at 60 standard cubic centimeters per minute (SCCM) and (B) 85 volume % Ar and 15 volume % O_2, flowing at 60 SCCM. endo, endothermic; wt %, weight percent. Under ambient pressures, CsH_2PO_4 dehydrates upon heating but reacts with neither hydrogen nor oxygen.

Materials Science, California Institute of Technology, Pasadena, CA 91125, USA.

*To whom correspondence should be addressed. E-mail: smhaile@caltech.edu

tioned over a broad dehydration process that peaks at 285°C. Under high pressure (*6*) or elevated water partial pressures (P_{H_2O}) (*7*), dehydration is largely circumvented and reproducible superprotonic behavior is observed, with a transition occurring at 230°C under atmospheric pressure. Thus, by retaining sufficient P_{H_2O} in a CsH_2PO_4-based fuel cell, reaction 1 can be suppressed and, in principle, superprotonic behavior of the electrolyte can be accessed. To this end, the onset of CsH_2PO_4 dehydration was measured under closed volume as a function of temperature (Fig. 2) (*4*). The data show that humidification of gases in liquid water at 70°C, with an equivalent P_{H_2O} of ~0.30 atm, is sufficient to prevent CsH_2PO_4 dehydration up to a temperature of ~270°C. Only slightly greater water partial pressures are required to suppress dehydration at a temperature as high as 346°C, the melting point of CsH_2PO_4 (*8*).

To demonstrate the viability of using moderate water partial pressures to provide thermal stability to a chemically stable solid acid, a membrane electrode assembly (MEA) was prepared with a 260-μm-thick CsH_2PO_4 electrolyte and a Pt electrocatalyst at both electrodes (*4*). The cell was operated under H_2/O_2 configuration at 235°C, in which both the anode and cathode gases were humidified (P_{H_2O} = 0.30 atm); humidification was essential to prevent dehydration of the CsH_2PO_4 electrolyte (*4*). Electrical current (100 mA cm^{-2}) was drawn continuously for 100 hours, after a 24-hour equilibration period, and polarization curves were collected both before and after long-term examination (Fig. 3).

During the continuous measurement, the cell showed remarkable stability; the voltage very gradually increased from 0.441 to 0.462 V, with an average of 0.460 V. The water that evolved at the cathode was in correspondence with that expected from drawing 100 mA cm^{-2} current (fig. S2) (*4*). The polarization curves obtained before and after the long-term evaluation were almost indistinguishable. The open-cell voltage (OCV) was 1.003 V for both measurements, a value somewhat lower than the theoretical OCV (Nernst potential) of 1.15 V for this cell. The difference between the theoretical and measured values is attributed to small leaks across the fuel cell seals and possible microcracks within the electrolyte. The peak power and maximum current densities remained similarly constant during the 100-hour stability test at 48.9 mW cm^{-2} and 301 mA cm^{-2}, respectively. Performance limitations were primarily due to electrolyte resistance, i.e., ohmic losses; decreasing the electrolyte thickness would be expected to increase the performance by up to a factor of 10 (fig. S3) (*4*). These power and current density values are about five times as high as those

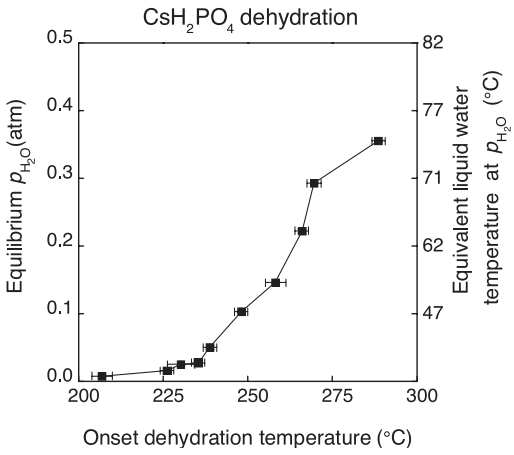

Fig. 2. Onset dehydration temperature of CsH_2PO_4 at 10 different equilibrium water partial pressures. The right axis corresponds to the equivalent liquid-vapor equilibrium temperature of water at the water partial pressure (P_{H_2O}) indicated at the left. Each onset dehydration temperature was identified by a discontinuous change in the slope of water partial pressure versus temperature upon heating CsH_2PO_4 to 300°C at 0.4°C min^{-1} at constant volume (fig. S4) (*4*).

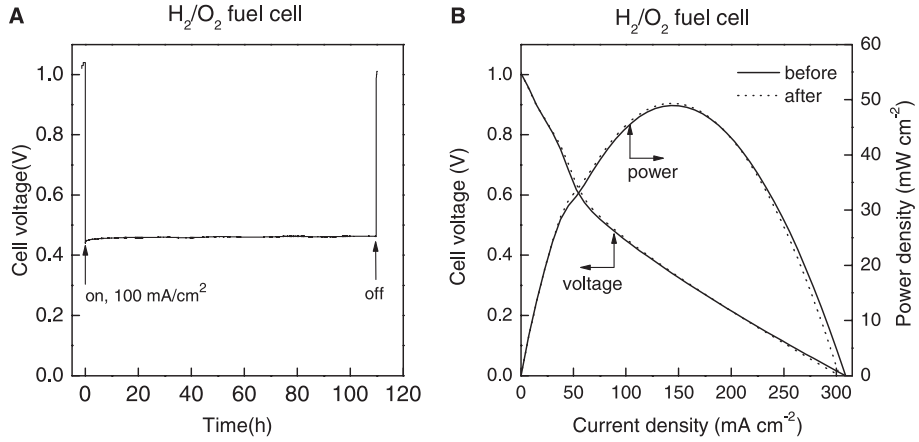

Fig. 3. H_2/O_2 fuel cell performance with the CsH_2PO_4-based electrolyte. (**A**) Cell voltage and water partial pressure as a function of time, while drawing 100 mA cm^{-2} continuous current for 100 hours. (**B**) Cell voltage and power density versus current density before and after the measurement at 100 hours. The cell was operated at 235°C under humidified H_2 and O_2 gases flowing at 50 SCCM at the anode and the cathode, respectively. Electrolyte thickness was 260 μm and catalyst loading was 18 mg cm^{-2} Pt. P_{H_2O} = 0.30 atm.

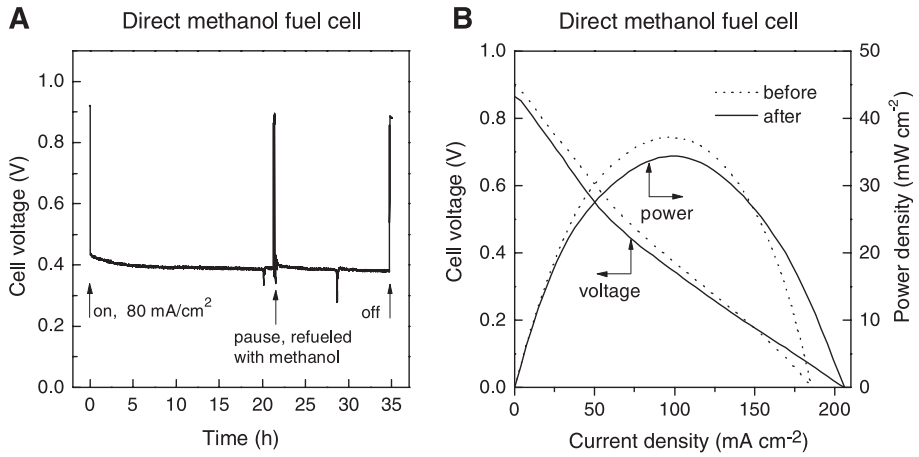

Fig. 4. DMFC performance with the CsH_2PO_4-based electrolyte. (**A**) Cell voltage as a function of time, while drawing 80 mA cm^{-2} of current for 35 hours. (**B**) Cell voltage and power density versus current density before and after the measurement at 35 hours. The cell was operated at 243°C. Gases fed to the anode and cathode were, respectively, CH_3OH, H_2O, and Ar (23:25:52 mol %), flowing at a total rate of 97 SCCM, and O_2 and H_2O (67:33 mol %), flowing at a total rate of 75 SCCM. After 21 hours, the measurement was paused to replenish the methanol supply. Electrolyte thickness was 260 μm and catalyst loadings were 13 mg cm^{-2} PtRu (50:50 mol %) at the anode and 15 mg cm^{-2} Pt at the cathode.

reported earlier for $CsHSO_4$, in which the membrane thickness was ~1.4 mm (*2*).

A second type of MEA was constructed with PtRu [50:50 mole percent (mol %)] as the anode electrocatalyst to demonstrate the viability of a CsH_2PO_4 electrolyte in vapor-fed DMFCs (*4*). Such fuel cells are anticipated to provide the advantages of complete impermeability of the electrolyte to methanol and elevated operating temperatures. These features, in turn, translate into higher power densities, higher CO tolerance, and, ultimately, lower precious metal catalyst loadings. We introduced vapor-phase methanol and water (0.92:1 molar ratio) into the anode compartment by using argon as a carrier gas, while humidified oxygen was fed into the cathode. The cell was operated at 243°C. Electrical current (80 mA cm^{-2}) was drawn continuously for 35 hours (without an initial equilibration step) and polarization curves were obtained both before and after the measurement (Fig. 4). As in the case of the H_2/O_2 cell, the methanol cell showed remarkable stability, with the voltage decreasing slightly from an initial value of 0.441 V to a final value of 0.381 V; the majority of that decrease occurred in the first few hours and is attributed to slight evolution of the electrocatalyst layer. Moreover, the two polarization curves are again quite similar. Peak power densities were 37.2 and 34.4 mW cm^{-2}, respectively, for the two measurements. Open-circuit voltages, measured at 0.897 and 0.865 V before and after stability examination, respectively, cannot be compared to a theoretical (Nernst) potential because, as is typical for DMFCs, the partial pressures of the product gas, CO_2, and possible intermediates, such as CH_4, were not controlled or monitored. Nevertheless, the OCVs are greater than those obtained from polymeric DMFCs (~0.8 V) (*9*, *10*), presumably because of the higher methanol content used here and the lower membrane permeability. The power densities reached in this work are within about a factor of 5 of the most advanced DMFCs (100 to 200 mW cm^{-2}) (*9*, *10*).

Despite the apparently poor thermal stability of CsH_2PO_4 in its superprotonic phase, both H_2/O_2 and DMFCs based on this material show excellent long-term performance when stabilized with water partial pressures of ~0.30 atm, depending on the temperature of operation. These "humidity-stabilized" solid acid fuel cells exhibit higher OCVs than polymer electrolyte fuel cells and thus may ultimately yield better overall system efficiencies. More important, the high-temperature operation and the much less demanding humidification requirement lead to system simplifications.

References and Notes

1. A. I. Baranov, L. A. Shuvalov, N. M. Shchagina, *JETP Lett.* **36**, 459 (1982).
2. S. M. Haile, D. A. Boysen, C. R. I. Chisholm, R. B. Merle, *Nature* **410**, 910 (2001).
3. R. B. Merle, C. R. I. Chisholm, D. A. Boysen, S. M. Haile, *Energy Fuels* **17**, 210 (2003).
4. Materials and methods are available as supporting material on *Science* Online.
5. B. M. Nirsha *et al.*, *Russ. J. Inorg. Chem.* **27**, 770 (1980).
6. D. A. Boysen, S. M. Haile, H. Liu, R. A. Secco, *Chem. Mater.* **15**, 727 (2003).
7. J. Otomo, N. Minagawa, C. Wen, K. Eguchi, H. Takahashi, *Solid State Ionics* **156**, 357 (2003).
8. E. Rapoport, J. P Clark, P. W. Richter, *J. Solid State Chem.* **24**, 423 (1978).
9. A. K. Shukla, C. L. Jackson, K. Scott, R. K. Raman, *Electrochem. Acta* **47**, 3401 (2002).
10. S. C. Thomas, X. M. Ren, S. Gottesfeld, P. Zelenay, *Electrochem. Acta* **47**, 741 (2002).

11. Supported by the NSF, Division of Materials Research, and the Office of Naval Research, Office of Electrochemical Power, Science, and Technology.

Supporting Online Material

www.sciencemag.org/cgi/content/full/1090920/DC1
Materials and Methods
SOM Text
Figs. S1 to S4
Table S1
References and Notes

28 August 2003; accepted 12 November 2003
Published online 20 November 2003;
10.1126/science.1090920
Include this information when citing this paper.

Osmium Isotope Heterogeneity in the Constituent Phases of Mid-Ocean Ridge Basalts

Abdelmouhcine Gannoun,[1*] Kevin W. Burton,[1] Louise E. Thomas,[1] Ian J. Parkinson,[1] Peter van Calsteren,[1] Pierre Schiano[2]

Radiogenic isotope variations in mid-ocean ridge basalts (MORB) are commonly attributed to compositional variations in Earth's upper mantle. For the rhenium-osmium isotope system, constituent MORB phases are shown to possess exceptionally high Re/Os (parent/daughter) ratios, consequently radiogenic ^{187}Os is produced from the decay of ^{187}Re over short periods of time. Thus, in the absence of precise age constraints, Os isotope variations cannot be unambiguously attributed to their source, although Re–Os isotope data for constituent minerals can yield crystallization ages, details of equilibration, and initial Os isotope values that relate directly to the mantle source.

The decay of ^{187}Re to ^{187}Os provides an exceptional tracer of recycled crustal materials in Earth's mantle. This is because oceanic and continental crust possess high Re/Os ratios, and develop radiogenic Os isotope compositions over time, which in turn can be readily traced as recycled material if mixed back into the convective mantle (*1*–*5*). MORB are believed to form by partial melting of Earth's upper mantle, and their concentration ratios of incompatible elements or radiogenic isotope compositions are considered to relate directly to the mantle source. A fundamental assumption underlying the use of radiogenic isotopes in such mantle-derived basalts is that they are in equilibrium with their mantle source (*6*, *7*). Thus, the composition of long-lived isotopes of heavy elements in MORB and the upper mantle should be the same. It is also assumed that the constituent phases of the basalts preserve isotope compositions that relate directly to the mantle source. For lithophile elements, such as Sr or Nd, parent/daughter ratios in MORB phases are relatively low such that shifts in the radiogenic isotope composition cannot be produced in less than 10^3 million years (My) (*8*). Thus, any variations in Sr and Nd isotope composition are commonly attributed to a compositional heterogeneity in the upper mantle (*8*). However, for the Re–Os isotope system silicate phases [such as olivine (*9*) and glass (*3*)] possess high $^{187}Re/^{187}Os$ (parent/daughter) ratios. This raises the possibility that radiogenic ^{187}Os can be produced in situ from the decay of ^{187}Re over short periods of time [i.e., 100 thousand years (ky) or less] (*5*). Consequently, the Os isotope composition of constituent phases in MORB may be variable depending on their Re/Os ratio and the time that has elapsed since crystallization. If the magmatic phases are in equilibrium, then they may yield an isochron that will give the age of crystallization, and the initial Os isotope composition defined by that best-fit line corresponds to that of the mantle source. However, if some of the phases were assimilated from previously solidified basalts or contaminated by seawater, then they may possess different isotope information to that of their basalt host or other phases. Thus, understanding the nature of the Re–Os isotope information preserved in MORB requires

[1]Department of Earth Sciences, The Open University, Walton Hall, Milton Keynes, MK7 6AA, UK. [2]Laboratoire Magmas et Volcans, Université Blaise-Pascal, 5 Rue Kessler, 63038 Clermont-Ferrand, France.

*To whom correspondence should be addressed. E-mail: a.gannoun@open.ac.uk